6 Particle Physics at DESY/HERA (H1)

J. Becker, Ilaria Foresti, S. Hengstmann (until 4/01), M. Hildebrandt, N. Keller, J. Kroseberg, Katharina Müller, P. Robmann, F. Sefkow, U. Straumann, P. Truöl, M. Urban, R. Wallny (until 4/01) and Nicole Werner

in collaboration with:
R. Eichler, W. Erdmann, C. Grab, M. Hilgers, B. List, S. Lüders, D. Meer and A. Schöning, Institut für Teilchenphysik der ETH, Zürich, S. Egli, K. Gabathuler, J. Gassner, and R. Horisberger, Paul–Scherrer–Institut, Villigen, and 34 institutes outside Switzerland

(**H1**–Collaboration)

6.1 Electron proton collisions at up to 320 GeV center of mass energy: overall status of the project

Since September 2000 no new data have been collected by the H1-experiment, because even after the conclusion of the long shutdown for the upgrade of the detector and the accelerator in July 2001, no useful collisions have been observed so far. The tuning of the positron and proton accelerators turned out to be more troublesome then expected, as we will report below (Sec.6.2). Consequently, also the status of those H1-components which have undergone an upgrade remains largely untested under realistic, high intensity conditions. However, after conclusion of the major effort, which was undertaken to optimize the calibration and alignment of tracker components (see Sec.6.5) near the end of 2001, finally the first results are emerging from the reprocessed 1999/2000 data ($\mathcal{L} = 91\text{pb}^{-1}$). Despite this most of our publications use data taken before 1999 ($\mathcal{L} = 50\text{pb}^{-1}$). In 18 publications ([1]-[18]) and 21 papers contributed to the 2001 high-energy conferences ([20]-[40]) of the collaboration the following principal areas are covered:

- neutral and charged electroweak current cross sections, proton structure functions and parton densities (extensions into the lower and higher Q^2 regimes, longitudinal structure function and use of radiative events) [4, 5, 11, 20, 24, 25, 26, 37, 43, 44, 47],
- determination of α_s and its scale dependence (structure function analysis, dijets) [2, 4, 43, 44, 47],
- search for states outside the standard model (squarks, ν^*, leptoquarks, single top, odderons) [6, 10, 14, 22, 33, 34, 36],
- photoproduction (inclusive, dijets, $\rho, J/\Psi$, $Q\bar{Q}$) [7, 16, 21, 30, 32, 38, 40],
- parton-fragmentation into multijet final states [1, 2, 3, 8, 15, 16, 31, 40],
- photo- and electroproduction of exclusive final states ($\rho, J/\Psi, \Psi'$) [21, 23, 27, 30],
- production of heavy quark-antiquark states ($Q\bar{Q}$) and of open charm and beauty [12, 13, 46, 38, 39, 41, 42, 45],
- diffractively produced final states (inclusive, D^*, jets, $\rho, J/\Psi, \Psi'$) [3, 13, 17, 18, 21, 23, 28, 29, 30, 31],
- virtual Compton scattering [9].

We will report below on the analyses in the heavy quark sector (sections 6.6.2 and 6.6.4), an area where there is manifest activity of the University of Zürich group (F. Sefkow's habilitation project and theses of J. Kroseberg and I. Foresti), in prompt photon production

(Sec.6.6.3, K. Müller's habilitation project) and also give a brief overview of the general status (Sec.6.6.1). Two Zürich analysis projects which are not discussed in detail concern QED Compton scattering (thesis N. Keller) and high Q^2 data (thesis N. Werner).

Besides the physics analysis the commissioning of our contributions to the upgrade program of the H1-detector occupied most group members (see Sec.6.4).

6.2 Status of the HERA accelerator

At an H1-meeting in February 2002 F. Willeke reported on the progress of the commissioning of the HERA accelerator complex. First collisions were registered by the H1 luminosity detector in September 2001. While collisions at low beam intensities (I_e = 0.8 mA (e^+) and I_p = 12 mA) have been obtained in December 2001 with a specific luminosity $\mathcal{L}_{spec.} = 1.68 \cdot 10^{30}$ mA^{-2}cm^{-2}s^{-1} (84 % of the design value, three times pre-upgrade average value) and beam spot sizes of $\sigma_x \times \sigma_y \approx 150 \times 50$ μm^2, the synchrotron radiation backgrounds exceeded the values which allow to turn on the detectors at full currents by two orders of magnitude. The beam based alignment procedures near the interaction regions took much longer than originally envisioned, but the new beam lattice and optics are now relatively well understood and the influence of the detector fields (in the absence of compensation coils) is now manageable. The origins of the high synchrotron radiation backgrounds were traced to a magnet aperture 90 m before the interaction region and backscattering from a collimator behind H1 (in positron direction). New shielding masks were inserted between January and March 2002 to protect against this. Furthermore a broken beam tube support in a cold straight section of the proton ring was replaced during this period, which required breaking the vacuum. In April 2002 shortly after the time interval reported here, the commissioning procedures have restarted.

6.3 Status of the H1-detector

Figure 6.1 shows the H1-detector with those elements highlighted, which experienced modification or have been added. In forward direction the existing proton and neutron detectors at 106 m and 60 - 90 m, respectively are supplemented by a very forward proton spectrometer at 200 m, where the scattered proton and the circulating beam are already separated sufficiently. This will increase the acceptance for charmed meson and vector meson production for $|t| \leq 0.5$ GeV^2.

For high Q^2 events the track density in forward direction is quite high. The reconstruction of events in this region has therefore been quite difficult and had to rely primarily on calorimeter response. The former radial drift chamber and transition radiation detector modules in the forward tracker (FTD) have now been replaced by eight planar wire chambers giving greater redundancy and helping to resolve pattern recognition ambiguities. Five new planes of Si detectors were also inserted near the beam pipe to cover small scattering angles. The design is similar to that of the existing backward silicon detector (BST). In combination with the central silicon detector built by ETHZ/PSI/UZH the H1-detector will now have nearly 4π precision Si tracking coverage.

In the low Q^2 backward region new proportional chambers have replaced the backward drift chamber, and the geometry of the time-of-flight scintillators has been adapted to the new beam elements. The latter was also done in forward direction.

The two-layer inner proportional chambers (CIP) and the drift chamber (CIZ) built in Zürich have been replaced by a new five-layer proportional chamber (CIP2000) also built in Zürich. The aim of this change was to improve z-vertex triggering and track reconstruction at the trigger level, as well as the rejection of background events, as we reported last year.

The trigger scheme is based on a projective geometry of the pads along the z-axis, thus requiring a decreasing number of pads with increasing width from the inner to the outer layers. The increased number of readout channels required new readout [48] and trigger electronics [49]. ETHZ is also involved in the development of a fast track trigger derived from central jet chamber information, which will allow online invariant mass reconstruction and hence selective triggering on charm and beauty production enriched samples.

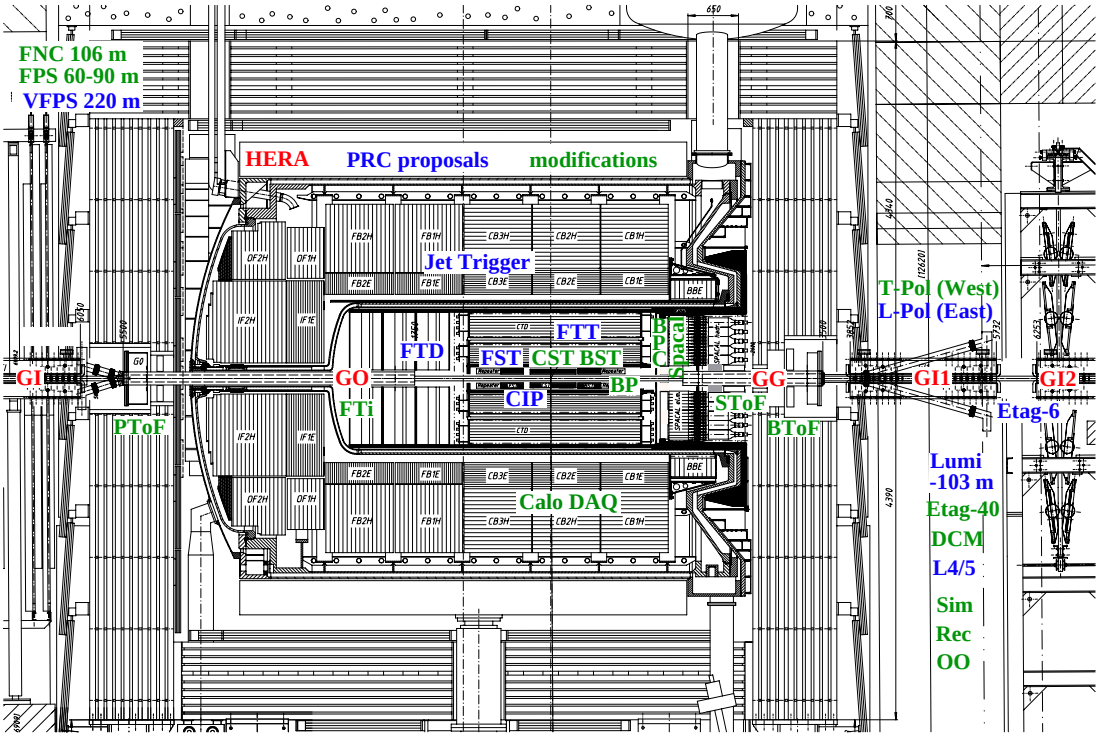

Figure 6.1: *The H1-detector after its 2000/2001 upgrade. New or modified detector elements are marked.*

6.4 Summary of group activities related to the H1-upgrade

The CIP2000 upgrade project is coordinated by the University of Zürich (U. Straumann) with ETH Zürich and University of Heidelberg as partners. The ASIC laboratory in Heidelberg developed the amplifier and readout chip CIPix, and the electronics for trigger and data acquisition is a common Heidelberg and Zürich University effort. ETH Zürich was responsible for all components dealing with the readout of the data at the detector end, and the transport to the electronic trailer via an optical transmission line with drivers and receivers at either end.

At the end of the two year construction period which involved up to five people in the workshops of our institute the CIP was transported to DESY in February 2001 and mounted inside the central tracker of H1. The readout prints and all other necessary supply connections have been mounted in April 2001. Figure 6.2 shows some aspects of the final test procedures in our laboratory in Zürich and of the installation steps in Hamburg.

For the z-vertex trigger the CIP2000 data are multiplexed fourfold and fed to 16 trigger cards, one per ϕ-sector. To cope with the enormous data rate a highly parallel system had to be developed. It is realised in large FPGA's (Altera APEX 20k400) with internal dual ported

• *CIP2000 after completion in the laboratory in Zürich.*

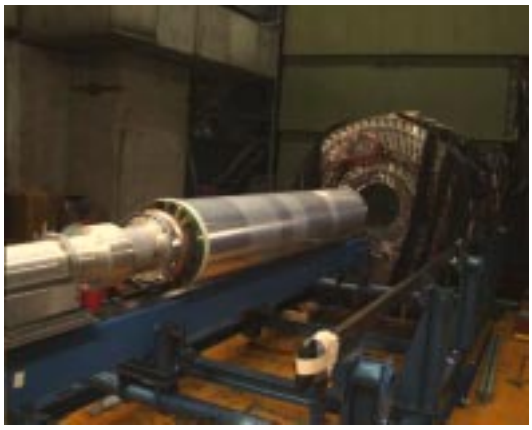

• *CIP2000 is prepared for insertion into the H1 central tracker.*

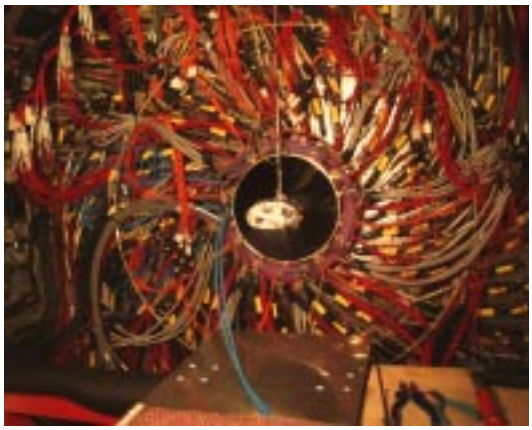

• *The H1 central tracker in its final position within the H1 detector seen from the backward (incoming proton) side with the electronics, gas and cooling lines connected (May 2001).*

• *On-chamber electronics is being mounted for tests in Zürich.*

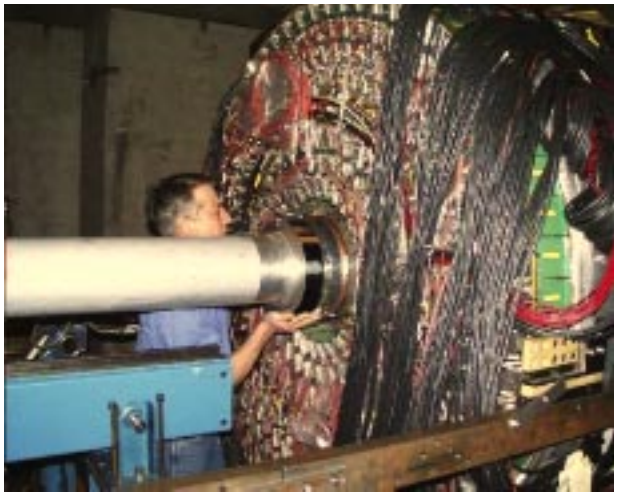

• *CIP2000 is in place.*

• *A CIP2000 trigger card.*

Figure 6.2: *Some aspects of the test procedures in our laboratory in Zürich and of the installation in Hamburg.*

memory. A trigger card is shown in Figure 6.2. The memory is used as a pipeline for the data of the CIP2000 for 21 bunch crossings while the trigger decision is being made. The latter proceeds in three consecutive steps. First tracks are reconstructed from the hits in the $\approx 10^4$ pads, then a z-vertex histogram is built, and finally a trigger decision is made. The system can cope with inefficient areas of a chamber or missing layers. The stored data are transfered via VME bus to the H1 storage bank systems. Therefore a DAQ system with fast inhomogeneous bus systems was developed. The whole system is now complete and has passed its initial tests successfully. The total data throughput of the system is 108 GBytes/s (!). For the system 25'000 lines of code in a special hardware description language (verilog) had to be written. The design and implementation of this trigger is the thesis project of M. Urban [49]. The development of the CIP2000 data acquisition system is a task included in the thesis project of J. Becker [50], while slow control (i.e. chamber HV and current as well as temperature monitoring and control), and on-line monitoring of the chamber efficiency is part of the thesis project of N. Werner. These different tasks necessary for the full integration of CIP2000 into H1 are being coordinated by M. Hildebrandt. Since the old z-vertex trigger allows to calculate the z-vertex histograms with a certain momentum threshold, it is planned to include it into the system, too. The necessary interface cards necessary are being developed.

In July 2001 first tests with cosmic muons were possible with the H1-detector closed and in beam position. Using the OR-signal, which is available from the 16 pads served by each CIPix readout chip, and a combination of two layers of proportional chambers in each of its 16 ϕ sectors, a cosmic muon trigger was created from the chamber itself. This initial test confirmed the satisfactory chamber performance measurements in the laboratory in Zürich, but also pointed to a variety of problems related to insufficient cooling. The ambient temperature produced by the central jet chamber electronics is so high, that the CIPix reaches temperatures near 50°C with the normal cooling circuit running at 17°C. At these temperatures instabilities in the addressing of some CIPix chips occurred at first, and later a complete loss of their functionality can be observed. A subsequent laboratory test confirmed that at these high temperatures wires bonded to the chips can break, which explains the loss of connection. As a counter measure a separate cooling circuit was installed with an operating temperature of 8°C, which will keep the CIPix temperature below 40°C. However, out of the five chamber layers the outermost two were partly lost before the roots of the problem were discovered. Furthermore three of the 24'000 anode wires are broken, and a few ϕ sectors in the remaining three planes are missing, too. However, the inner three chambers and the trigger derived from them still cover the complete solid angle and can be operated, requiring a coincidence of at least two cathode pads on a track. The whole frontend electronics is presently being rebuilt in such a way, that the bond breaking can no longer occur, and during the next short shutdown a replacement is planned. Furthermore additional cooling lines will then be added to the chamber electronics.

Since August 2001 the data acquisition has been completed, such that each individual pad of the whole chamber can now be read out. Events are correctly stored and displayed, and the readout timing has been adjusted within one bunch crossing to the central data acquisition system. The correct trigger algorithm based on pad information and tracks has been written, and was implemented on the FPGA's and tested. For the fine tuning of course real collisions are awaited. Four trigger elements are foreseen: correct event timing ($T0$), vertex in the interaction region, background from upstream or from downstream of the interaction region. The temperature monitoring is installed and if a limit is exceeded the supply voltages will be automatically switched off.

6.5 Reprocessing for optimal tracking performance

Last year we reported on the collaboration-wide effort to optimize the performance of the H1 tracking system. Using the additional redundancy provided by the central silicon tracker (CST) and new mathematical procedures, the calibration of individual components, as well as their overall consistency has been considerably improved; such that the obtained tracking resolution now corresponds to the design goals. Although this initiative was primarily directed towards achieving optimal vertexing precision which is so crucial for tagging heavy quarks by means of their lifetime signature, momentum and angular resolution benefited as well. As a consequence, the signal quality of invariant mass peaks also improved significantly. To illustrate this, in Figure 6.3 the D^* signal in the "golden" decay mode $D^* \to K\pi\pi$, is shown, as it has been obtained before and after the new reconstruction. Meanwhile all data taken

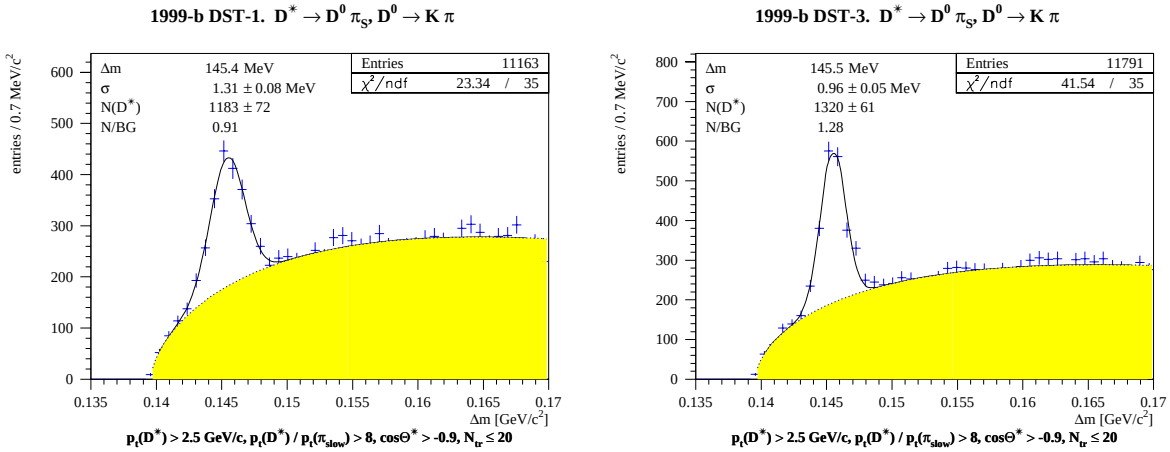

Figure 6.3: *D^* signal in the mass difference distribution $\delta m = m(K\pi\pi) - m(K\pi)$ before and after reprocessing the data with new alignment and calibration.*

from 1997 to 2000 have been reprocessed, and similar improvements are observed for all running periods. With the "Tracking Task Force" thus successfully terminated, F. Sefkow, who led the team for the past 2 years, has switched over to act as new convenor of the Heavy Flavour physics working group in H1, which looks forward to exploiting the potential offered by the improved precision and statistics of the data. In paticular the studies of charm and beauty production depend heavily on the tracking performance, and in this area the largest fraction of the HERA data still waits to be analyzed.

6.6 Results from recent analyses

6.6.1 *ep* collisions at high energies

Progress in our understanding of proton structure in the last few years is closely linked to the improved accuracy and larger kinematic extent of the measurements from the two experiments H1 and ZEUS at the electron- or positron-proton collider HERA. In conjunction with older fixed target muon and neutrino data these new data are used to determine quark and gluon densities within the proton through analysis of their QCD evolution.

To briefly introduce the terminology, we recall that the differential cross section for deep inelastic positron (electron) proton scattering, if only the neutral electromagnetic current

(virtual photon (γ) and boson (Z^0) exchange) is considered, takes the following form:

$$\frac{d^2\sigma_{NC}}{dx\ dQ^2} = \frac{2\pi\alpha^2}{xQ^4}\Phi_{\gamma,Z}(x,Q^2) = \frac{2\pi\alpha^2}{xQ^4}\left[Y_+\tilde{F}_2(x,Q^2) \mp Y_- x\tilde{F}_3(x,Q^2) - y^2\tilde{F}_L(x,Q^2)\right] .$$

The *structure function term* $\Phi_{\gamma,Z}(x,Q^2)$ is a linear combination of the dominant $\tilde{F}_2$ structure function, the longitudinal structure function $\tilde{F}_L$, and the $x\tilde{F}_3$ structure function which in the standard model is significant only when Q^2 is sufficiently large to render Z^0 exchange non-negligible. $Q^2 \equiv -t$ is the squared four-momentum transfer of the scattered positron and x the fraction of the proton momentum carried by the struck quark. The variable y is defined as $y = Q^2/xs$, with $\sqrt{s}$ being the total positron-proton center of mass energy. In a Lorentz frame where the proton is at rest, y measures the energy transfer of the positron. The kinematical range covered at HERA is compared with that of fixed target experiments in Fig.6.5. Reaching $Q^2 \approx 10^5$ GeV^2 corresponds to a spatial resolution in the am range.

One of the main goals of the HERA physics program is the determination of the three structure functions. Since both the positron and the final state hadrons marking the path of the struck quark are observed in the detector the kinematical variables can be reconstructed from angle and energy of either positron or hadronic jet or a combination of both. For example in terms of positron quantities one finds

$$y_e = 1 - \frac{E_e(1-\cos\theta_e)}{2E_e^0} , \quad Q_e^2 = \frac{E_{T,e}^2}{1-y_e} , \quad M_e = \sqrt{sx_e} = \sqrt{\frac{Q_e^2}{y_e}} .$$

M_e is the mass of the positron-quark system, $E_{T,e}$ the transverse energy of the positron, $E_e^0 = 27.5$ GeV and θ_e is the polar scattering angle relative to the proton direction. The H1-detector has good positron energy resolution, which favors use of positron variables in particular at high momentum transfers, but important and quite accurate cross checks using the jet quantities are possible, too.

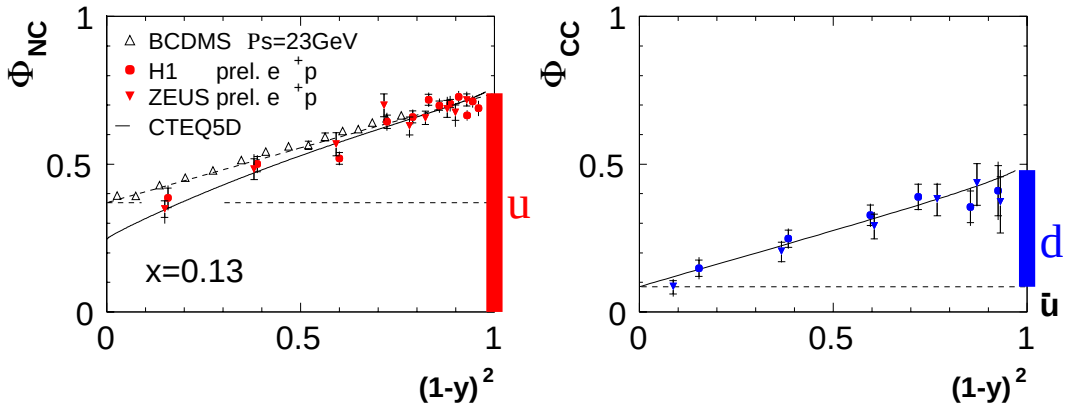

Figure 6.4: *Structure function terms* $\Phi_{NC} \equiv \Phi_\gamma$ *and* $\Phi_{CC} \equiv \Phi_W$ *for* e^+p *scattering at* $x = 0.13$ *as a function of* $(1-y)^2$ *(taken from [51]).*

For the charged electroweak current mediated by W-boson exchange the cross section takes the form

$$\frac{d^2\sigma_{CC}}{dx\ dQ^2} = \frac{G_F^2}{2\pi x}\left(\frac{M_W^2}{M_W^2+Q^2}\right)^2 \Phi_W(x,Q^2) .$$

In leading order QCD the structure function terms take a particularly instructive form which

exhibits the valence (u, d) and sea quark (s, c) densities within the proton

$$\Phi_\gamma = \left(1 + (1-y)^2\right)\left[\frac{4}{9}(u + c + \bar{u} + \bar{c}) + \frac{1}{9}(d + s + \bar{d} + \bar{s})\right]$$

$$\Phi_W = x\left[(\bar{u} + \bar{c}) + (1-y)^2(d + s)\right] \quad (e^+) \quad ; \; \Phi_W = x\left[(u + c) + (1-y)^2(\bar{d} + \bar{s})\right] \quad (e^-) \quad .$$

The valence quark contributions can be identified through their dependence on $(1-y)^2$ equivalent to $\cos^4(\theta^*/2)$, where θ^* is the scattering angle in the eq centre-of-mass system (Fig.6.4).

Figure 6.5 displays the positron proton cross section at high momentum transfer and indicates nicely the electroweak unification scale of $Q^2 \approx 10^4$ GeV^2 (near equality of the charged and neutral current cross sections), and the agreement between the data from the two collider experiments as well as with standard model predictions. The latter agreement holds also for all observables sensitive to signals of beyond the standard model physics. The lower limits (95% confidence) on the quark radius assuming point-like leptons ($f_e \equiv 1$: $R_q < 0.82$ am (10^{-18}m) or common form factors ($f_e = f_q$: $R_q < 0.57$ am) may be cited [52] as just one example for the various exclusion limits set by our data [6, 10, 14, 35, 36, 52].

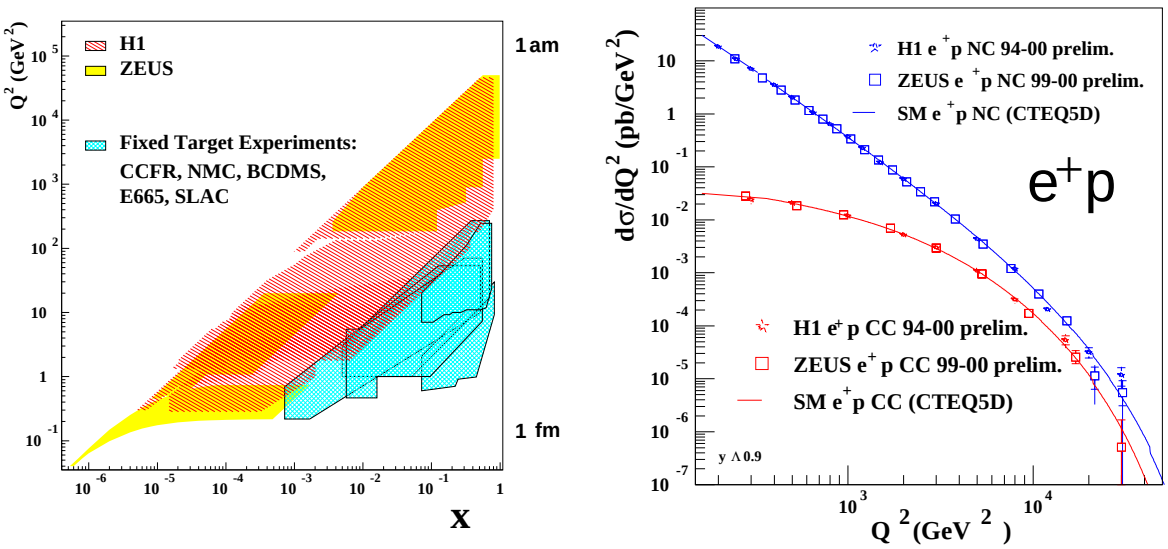

Figure 6.5: *Left: Kinematic reach of deep inelastic scattering experiments in the x versus Q^2 plane [51]. Right: Positron-proton charged and neutral current cross section integrated over all parton momenta x in function of the momentum transfer Q^2. The data come from both HERA collider experiments* [P52] *[51].*

6.6.2 Beauty cross section

Beauty production recently received renewed interest, also due to the new measurements at HERA, which were in the focus of discussions on QCD tests at last year's summer conferences. The results [41, 45, 53] are summarized in Fig. 6.6a.

Thanks to the central silicon tracker H1 is leading the field in this area. The lifetime-based results are unique at HERA and currently being finalized for publication (Thesis J. Kroseberg). Similar discrepancies between data and theory have been observed in $\bar{p}p$ collisions, and more recently, also in two-photon interactions at LEP (for a short review, see [41]). Deep-inelastic ep scattering provides, apart from e^+e^- annihilations, the cleanest environment for

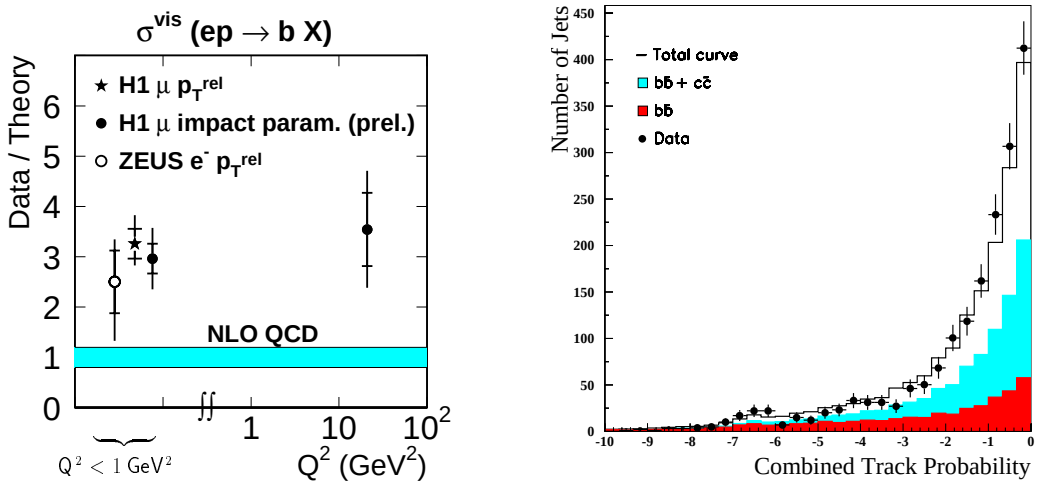

Figure 6.6: *Left: ratio of b production cross sections measured at HERA over theoretical expectation, as a function of Q^2. Right: distributions of a vertex estimator for data and simulated $b\bar{b}$, $c\bar{c}$ and light quark events. Small values indicate the presence of tracks from secondary decay vertices.*

the study of beauty production, since uncertainties associated with hadronic structure are limited to the well-measured proton. Studies of the process at HERA therefore hold the promise to provide clues to resolve this puzzle.

In order to obtain more information on the production dynamics, it is necessary to tag the rarely produced b quarks with highest possible efficiency. Multi-impact parameter methods based on the lifetime signature in inclusive decay modes have been successfully applied at other experiments and hold the promise to bear fruit also at HERA, since the achieved track and vertex resolutions are similar to, e.g., what is available at LEP. The idea is to combine the significances with which extrapolated tracks miss the ep interaction point such that one obtains a probability which quantifies whether an event or a jet originates from one common primary vertex, or contains secondary vertices from heavy quark decays. The discriminating power of an estimator constructed along these lines is illustrated in Fig.6.6b taken from ongoing analysis work (thesis I. Foresti).

We are using here a muon-tagged dijet sample, on which our previous measurements are based, such that the beauty content is under control. This allows the tagging efficiency to be calibrated for a subsequent application of the method to the general case of an unbiased jet selection.

6.6.3 Prompt photon production

Besides deep-inelastic scattering at HERA also reactions of high energy photons with the proton can be studied (γp collisions).

During the last years the research concentrated on the structure of the virtual photon, and on the determination of an effective parton distribution in the photon based on the measurement of di-jet events.

With the large luminosity of 133 pb^{-1} collected in the years 96-00 it is now possible to study the structure of the photon in more detail by analysing events with isolated high energetic photons. Events with a hard photon (prompt photon) instead of a gluon emitted in the hard subprocess depend much less on details of the fragmentation or hadronisation. As a result the systematic error in the determination of the momentum fraction of the partons

of the scattering process is reduced considerably.

The cross section of the direct process $q\gamma \rightarrow q\gamma$ where the virtual photon takes part in the scattering process is 197 pb. Relevant for the determination of the photon structure is the resolved process, where a parton from the photon scatters off a parton from the proton. The dominant resolved process $qg \rightarrow q\gamma$ has a cross section of 273 pb, the process $q\bar{q} \rightarrow g\gamma$ is strongly suppressed with a cross section of only 40 pb. The resolved process is further suppressed kinematically, since the scattered photon is pointing in forward direction (direction of the proton beam). In forward direction the identification of the photon is hampered by multiple scattering and conversion due to dead material and particles from the proton remnant.

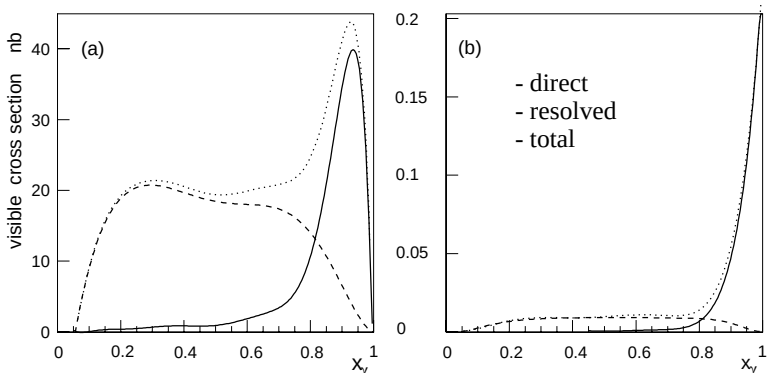

Figure 6.7: *Visible cross section for (a) two jet events and (b) events with prompt photons as a function of x_γ the momentum fraction of the photon carried by the parton. The full line shows the contribution of the direct process, the dashed line from the resolved process and the dotted line the sum of both.*

The disadvantage of this analysis is the low cross section which is suppressed by a factor of the order of $\mathcal{O}(\alpha/\alpha_s)$ with respect to the two jet production (see Fig.6.7). Therefore, the crucial point of the analysis is the identification of background from di-jet production in photoproduction events with high transverse momenta. The particles which mimic a photon candidate are mainly neutral mesons (π^0 or η).

The transverse and longitudinal cluster size is used to suppress these events but is not sufficient to separate signal and background. A further cut on the isolation of the photon, which also reduces higher order processes such as events with a photon radiated off the outgoing quark, has to be applied. It reduces the background to roughly 25% but cuts also significantly into the signal for resolved photons.

Further discrimination of neutral mesons and photons on a statistical basis need a detailed understanding of the shower shapes both in data and in Monte Carlo. The standard Monte Carlo description is not sufficient so it was necessary to start a detailed though time consuming simulation both for the signal and the background contribution. Preliminary results are expected this summer.

6.6.4 Inelastic J/Ψ production

Also in the second branch of heavy flavour physics, in heavy quarkonium production, H1 recently arrived at new, leading results based on large statistics ($\sim 80\,pb^{-1}$), including most recent data. The J/Ψ meson with its clean experimental dilepton signature was originally thought to provide access to the gluon density in the proton in a similar manner as open charm production. However, measurements of charmonium production in $\bar{p}p$ collisions were

found in excess of predictions by one to two orders of magnitude and put the validity of the conventional QCD approach into doubt. In the theoretical description, additional production channels were introduced; the requirement that the bound $c\bar{c}$ state produced in the hard perturbative interaction must be left in a color-neutral (*color-singlet* CS) state was given up, *color-octet* (CO) states with net color-charge are in general expected to contribute as well. The Tevatron data can be described in this framework, however at the expense of new non-perturbative degrees of freedom, which describe the transition from the octet states into observable (color-neutral) hadrons. These parameters must be adjusted to experimental data, but are considered to be universal; a hypothesis which must withstand experimental verification.

HERA provides a formidable testing ground for these rather recent developments. The measured p_T spectrum of J/Ψ mesons recorded in photoproduction is compared to theoretical predictions in Fig.6.8. The events have triggered using track information from the CIP and CJC, in coincidence with a muon signal from the J/Ψ decay. The data extend to higher transverse momenta than previous measurements and thus provide a better lever arm to disentangle contributions with different p_T dependences. In fact, the reaction $\gamma p \to J/\Psi X$ is

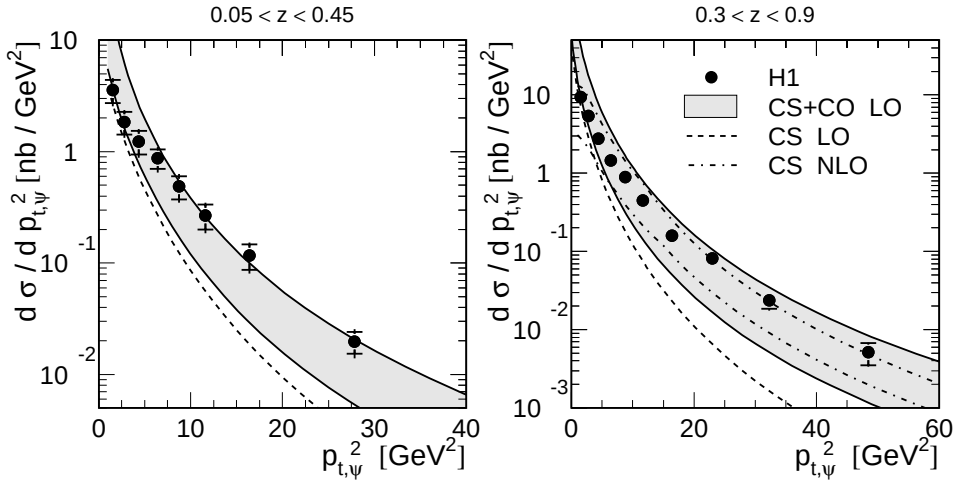

Figure 6.8: *p_T spectra of J/Ψ mesons, measured in photoproduction, compared with QCD predictions. The NLO calculation is not applicable at low values of the inelasticity z, where resolved photon processes become important.*

the only one for which a full next-to-leading order (NLO) computation has been performed, and the comparison shows that while a description including CS and CO contributions is compatible with the data, adding order α_s^2 corrections can change their relative importance considerably. The CO processes also exhibit different variations with photon virtuality Q^2; measurements in DIS therefore provide complementary information. The J/Ψ cross section as a function of Q^2 is displayed in Fig.6.9. The recent QCD calculation, shown for comparison, includes part of the NLO corrections and is expected to be more reliably for virtualities higher than the J/Ψ mass squared. The new data, with extended range and precision, are in fact better described as Q^2 increases. These measurements represent significant constraints to the further development of a unified QCD description of charmonium production in $\bar{p}p$, γp and ep interactions.

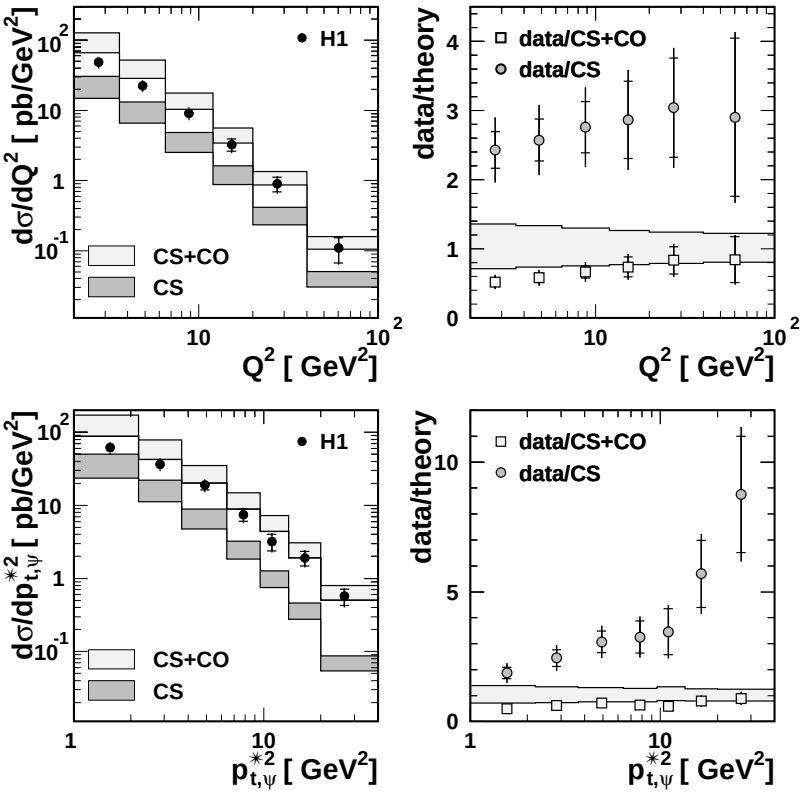

Figure 6.9: *J/Ψ production cross sections, measured in DIS as functions of Q^2 and of p_T^*, the transverse momentum in the hadronic centre-of-mass system, compared with QCD calculations.*

References

[1] *Di-jet Production in Charged and Neutral Current e^+p Interactions at High Q^2*, H1-Coll., C. Adloff *et al.*, Eur. Phys. J. **C19** (2001), 429

[2] *Measurement and QCD Analysis of Jet Cross Sections in Deep-Inelastic Positron-Proton Collisions at $\sqrt{s}$ of 300 GeV*, H1-Coll., C. Adloff *et al.*, Eur. Phys. J. **C19** (2001), 289

[3] *Diffractive Jet-Production in Deep-Inelastic e^+p Collisions at HERA*, H1-Coll., C. Adloff *et al.*, Eur. Phys. J. **C20** (2001), 29

[4] *Deep-Inelastic Inclusive ep Scattering at Low x and a Determination of α_s*, H1-Coll., C. Adloff *et al.*, Eur. Phys. J. **C21** (2001), 33

[5] *Measurement of Neutral and Charged Current Cross Sections in Electron-proton Collisions at High Q^2 at HERA*, H1-Coll., C. Adloff *et al.*, Eur. Phys. J. **C19** (2001), 269

[6] *Searches at HERA for Squarks in R-Parity Violating Supersymmetry*, H1-Coll., C. Adloff *et al.*, Eur. Phys. J. **C20** (2001), 639

[7] *Photoproduction with a Leading Proton at HERA*, H1-Coll., C. Adloff *et al.*, Nuclear Physics **B619** (2001), 3

[8] *Three-Jet Production in Deep-Inelastic Scattering at HERA*, H1-Coll., C. Adloff *et al.*, Phys. Lett. **B515** (2001), 17

[9] *First Measurement of the Cross Section for Deeply Virtual Compton Scattering*, H1-Coll., C. Adloff *et al.*, Phys. Lett. **B517** (2001), 47

[10] *A Search for Leptoquark Bosons in e^-p Collisions at HERA* , H1-Coll., C. Adloff *et al.*, Phys. Lett. **B523** (2001), 234

[11] *On the Rise of the Proton Structure Function F_2 towards Low x* , H1-Coll., C. Adloff *et al.*, Phys. Lett. **B520** (2001), 183

[12] *Measurement of $D^{*\pm}$-Meson Production and F_2^c in Deep-Inelastic Scattering at HERA*, H1-Coll., C. Adloff *et al.*, Phys. Lett. **B528** (2002), 199

[13] *$D^{*\pm}$ Meson Production in Deep-Inelastic Diffractive Interactions at HERA*, H1-Coll., C. Adloff *et al.*, Phys. Lett. **B520** (2001), 191

[14] *Search for Excited Neutrinos at HERA* , H1-Coll., C. Adloff *et al.*, Phys. Lett. **B525** (2002), 9

[15] *Measurement of Dijet Electroproduction at Small Jet Separation*, H1-Coll., C. Adloff *et al.*, Eur. Phys. J. **C** (2002), in print

[16] *Measurement of Dijet Cross Sections in Photoproduction at HERA*, H1-Coll., C. Adloff *et al.*, DESY 01 – 225, hep-ex 0201006, Eur. Phys. J. **C** (2002), in print

[17] *Energy Flow and Rapidity Gaps between Jets in Photoproduction at HERA*, H1-Coll., C. Adloff *et al.*, DESY 02 – 023, hep-ex 0203011, Eur. Phys. J. **C** (2002), in print

[18] *A Measurement of the t Dependence of the Helicity Structure of Diffractive ρ Meson Electroproduction at HERA*, H1-Coll., C. Adloff *et al.*, DESY 02 – 027, hep-ex/0203022, Phys. Lett. **B** (2002), in print

[19] Contr. to Int. Europhysics Conf. on High Energy Physics, Budapest, Hungary (July 2001), and to *Lepton-Photon 01*: XX. Int. Symp. on Lepton and Photon Interactions at High Energies, Rom (July 2001).

[20] *Inclusive Measurement of Deep Inelastic Scattering at High Q^2 in ep Collisions at HERA* (# 741, # 481, [19])

[21] *Diffractive $\Psi(2s)$ Photoproduction at HERA* (# 792, # 486, [19])

[22] *Investigation of Pomeron- and Odderon Induced Photoproduction of Mesons Decaying to Pure Multiphoton Final States at HERA* (# 795, # 488, [19])

[23] *Measurement of Density Matrix Elements for ρ Meson Production at Large $|t|$* (# 796, #489, [19])

[24] *A New Measurement of the Deep Inelastic Scattering Cross Section and of F_L at Low Q^2 and Bjorken-x at HERA* (#799, # 492, [19])

[25] *Measurement of the Proton Structure Function Using Radiative Events at HERA* (# 801, # 493, [19])

[26] *Radiative Charged Current Interactions at HERA* (#804, # 497, [19])

[27] *Diffractive J/Ψ Vector Meson Production at High t at HERA* (# 806, # 499, [19])

[28] *Measurement of the Diffractive Structure Function $F_2^{D(3)}(\beta, Q^2, x_{\P}$* (#808, # 500, [19])

[29] *Measurement of Semi-inclusive Diffractive Deep-inelastic Scattering with a Leading proton at HERA* (# 809, # 501, [19])

[30] *Photoproduction of ρ Mesons with a Leading Proton* (# 810, # 502, [19])

[31] *Dijet Cross Section in Photoproduction and Deep-inelastic Scattering with a Leading Neutron at HERA* (# 811, # 503, [19])

[32] *The Photoproduction of Protons at HERA* (# 815, # 507, [19])

[33] *Search for Compositeness, Leptoquarks and Large Extra Large Dimensions in eq Contact Interaction at HERA* (#785, # 479, [19])

[34] *Observation of Events with Isolated Leptons and Missing P_T and Comparison to W Production at HERA* (#802, #495, [19])

[35] *A Search for Leptoquark Bosons in ep Collisions at HERA* (#822, # 514, [19])

[36] *Search for Single Top Production in $e^+ - p$ collisions at HERA* (# 824, # 512, [19])

[37] *Inclusive Measurement of Deep Inelastic Scattering at High Q^2 in ep Collisions at HERA* (# 787,# 481, [19])

[38] *Measurement of the Beauty Photoproduction Cross Section* (# 790, # 483, [19])

[39] *Beauty Production in Deep Inelastic Scattering* (# 807, # 484, [19])

[40] *Measurement of Single Inclusive High E_T Jet Cross Sections in Photoproduction at HERA* (# 813, # 505, [19])

[41] *Open beauty production*, F. Sefkow, Proc. Workshop on New Trends in HERA Physics 2001, Ringberg Castle, Tegernsee, Germany (June 2001); hep-ex/0109038.

[42] *Open beauty production at HERA*, J. Kroseberg, hep-ex/0108052, Proc. 9^{th} Int. Workshop on Deep Inelastic Scattering (DIS 2001), Bologna, Italy, 27 Apr - 1 May 2001

[43] *The Gluon Distribution xg and the Strong Coupling Constant α_s from Inclusive DIS data by H1*, R. Wallny, Proc. 9^{th} Int. Workshop on Deep-Inelastic Scattering (DIS2001), Bologna, Italy (May 2001)

[44] *Measurement and QCD Interpretation of the Deep-inelastic ep Scattering Cross Section by H1*, R. Wallny , Proc. Int. Europhysics Conf. on High-Energy Physics (HEP 2001), Budapest, Hungary (July 2001), D. Horvath *et al.* eds., J. High-Energy Phys. Proc. Sect. (*http://jhep.sissa.it/*), PRHEP-hep2001/008

[45] *Heavy Quark Production in Deep-inelastic Scattering*, F. Sefkow, Proc. Int. Europhysics Conf. on High-Energy Physics (HEP 2001), Budapest, Hungary (July 2001), D. Horvath *et al.* eds., J. High-Energy Phys. Proc. Sect. (*http://jhep.sissa.it/*), PRHEP-hep2001/021, hep-ex/0110036.

[46] *Open Heavy Flavour Production at HERA*, J. Kroseberg, Proc. Lake Louise Winter Institute on Fundamental Interactions, Lake Louise, Alberta, Canada (February 2002)

[47] *Deep-Inelastic Inclusive ep Scattering at Low x and a Determination of α_s*, Rainer Wallny, PhD-thesis

[48] *Compact Frontend-Electronics and Bidirectional 3.3 Gbps Optical Datalink for Fast Proportional Chamber Readout*, S. Lüders *et al.* hep-ex 0107064, Nucl. Instr. Meth. **A** (2001), in print

[49] *Das Triggersystem der CIP Kammer bei H1*, Frühjahrstagung DPG, Leipzig (März 2001), available at *https://www.desy.de/ũrban/ftp/DPG%202002/H1_CIP2k_Triggersystem_DPG2002_140302.zip*

[50] See report given by J. Becker at DESY, November 2001, available at *http://www-h1.desy.de/b̃ecker/Documents/Trigger_Meeting_12_11_01.ps.gz*

[51] M. Erdmann, *Proton and photon structure*, Proc. Int. Symp. on Lepton and Photon Interactions at High Energies, Rome (July 2001), DESY 02 – 013.

[52] *Search for New Physics Phenomena in eq Contact Interactions at HERA*, H1-Coll., C. Adloff *et al.*, in preparation.

[53] C. Adloff *et al.* [H1 Collaboration], Phys. Lett. **B467** (1999) 156, erratum ibid. **B518** (2001) 331; J. Breitweg *et al.* [ZEUS Collaboration], Eur. Phys. J. **C18** (2001) 625.

[54] F. Abe *et al.* [CDF Collaboration], Phys. Rev. Lett. **79** (1997) 572; ibid. 578.

[55] G.T. Bodwin, E. Braaten and G.P. Lepage, Phys. Rev. **D51** (1995) 1125, erratum ibid. **D55** (1995) 5853; E. Braaten and Y.Q. Chen, Phys. Rev. **D54** (1996) 3216; W.E. Caswell and G.P. Lepage, Phys. Lett. **B167** (1986) 437.

[56] *Inelastic Photoproduction of J/Ψ Mesons at HERA*, H1-Coll., C. Adloff *et al.*, in preparation.

[57] *Inelastic Leptoproduction of J/Ψ Mesons at HERA*, H1-Coll., C. Adloff *et al.*, in preparation.